Developmental Cell
Article

EGF-Induced Centrosome Separation Promotes Mitotic Progression and Cell Survival

Balca R. Mardin,[1,5] Mayumi Isokane,[2] Marco R. Cosenza,[3] Alwin Krämer,[3] Jan Ellenberg,[2] Andrew M. Fry,[4] and Elmar Schiebel[1,*]
[1]Zentrum für Molekulare Biologie der Universität Heidelberg, DKFZ-ZMBH Allianz, Im Neuenheimer Feld 282, 69120 Heidelberg, Germany
[2]Cell Biology and Biophysics Unit, European Molecular Biology Laboratory, 69117 Heidelberg, Germany
[3]Clinical Cooperation Unit Molecular Hematology/Oncology, German Cancer Research Center (DKFZ) and Department of Internal Medicine V, University of Heidelberg, 69120 Heidelberg, Germany
[4]Department of Biochemistry, University of Leicester, Leicester LE1 9HN, UK
[5]Present address: Genome Biology Unit, European Molecular Biology Laboratory, 69117 Heidelberg, Germany
*Correspondence: e.schiebel@zmbh.uni-heidelberg.de
http://dx.doi.org/10.1016/j.devcel.2013.03.012

SUMMARY

Timely and accurate assembly of the mitotic spindle is critical for the faithful segregation of chromosomes, and centrosome separation is a key step in this process. The timing of centrosome separation varies dramatically between cell types; however, the mechanisms responsible for these differences and its significance are unclear. Here, we show that activation of epidermal growth factor receptor (EGFR) signaling determines the timing of centrosome separation. Premature separation of centrosomes decreases the requirement for the major mitotic kinesin Eg5 for spindle assembly, accelerates mitosis, and decreases the rate of chromosome missegregation. Importantly, EGF stimulation impacts upon centrosome separation and mitotic progression to different degrees in different cell lines. Cells with high EGFR levels fail to arrest in mitosis upon Eg5 inhibition. This has important implications for cancer therapy because cells with high centrosomal response to EGF are more susceptible to combinatorial inhibition of EGFR and Eg5.

INTRODUCTION

A critical event during mitosis is the assembly of the bipolar spindle. The mitotic spindle comprises two microtubule organizing centers (centrosomes), microtubules and kinetochores (Walczak and Heald, 2008). During spindle assembly, centrosomes organize microtubules that either interdigitate or attach to kinetochores (Tanenbaum and Medema, 2010). One of the earliest events during spindle assembly is the resolution of the centrosomal linker that holds the two centrosomes together during interphase. This can occur by one of two redundant pathways (Bruinsma et al., 2012; Mardin and Schiebel, 2012). First, the Mst2-hSav1-Nek2A module promotes the accumulation of Nek2A kinase at the centrosomes. Nek2A then phosphorylates the centrosomal linker proteins, C-Nap1 and rootletin, thereby inducing the dissolution of the linker. Second, the kinesin-5 motor protein Eg5 slides antiparallel microtubules apart creating a force that is able to separate the centrosomes even when the Mst2-hSav1-Nek2A pathway is impaired (Mardin et al., 2010). In addition to these two pathways, the timing of centrosome separation was suggested to be differentially regulated relative to nuclear envelope breakdown. In different cells, centrosome separation occurs either via the prometaphase pathway that depends on kinetochore generated forces or the prophase pathway that is independent of the kinetochores (McHedlishvili et al., 2012; Toso et al., 2009).

The motor protein Eg5 is important for bipolar spindle assembly and spindle elongation in anaphase. Eg5 inhibition or depletion halts mitotic progression in prometaphase (Kapoor et al., 2000; Mayer et al., 1999; Sawin and Mitchison, 1995). However, functional analysis of Eg5 is complicated by overlapping pathways that drive centrosome separation, spindle assembly and spindle elongation; the aforementioned Mst2-hSav1-Nek2A kinase module being a prime example. Additionally, it was recently shown that upregulation of the kinesin-12 hKlp2/Kif15 can generate cells that divide independently of Eg5 (Raaijmakers et al., 2012).

Thirty years ago, Sherline and Mascardo (1982) observed that addition of epidermal growth factor (EGF) to cells induced centrosome separation, however, the mechanisms behind this interesting phenomenon were unclear. EGF is well known to bind and activate ErbB-1 receptor tyrosine kinase, the epidermal growth factor receptor (EGFR), which has crucial roles in determining growth state and cancer development (Hynes and MacDonald, 2009). Importantly, EGFR is known to be mutated or differentially expressed in many tumor types thus constitutes one of the prime targets in cancer therapy (Klein and Levitzki, 2009). EGFR activates a number of intracellular pathways through several signal transducers (Hackel et al., 1999; Zwick et al., 1999). Although its potential in regulating cell proliferation via the control of G1/S transition is well established, whether EGFR signaling impacts upon mitosis is largely unknown.

In this study, we found that EGF induces early centrosome separation in S phase through activation of the Mst2-hSav1-Nek2A kinase module. Addition of EGF stimulates premature centrosome separation and drastically reduces the requirement

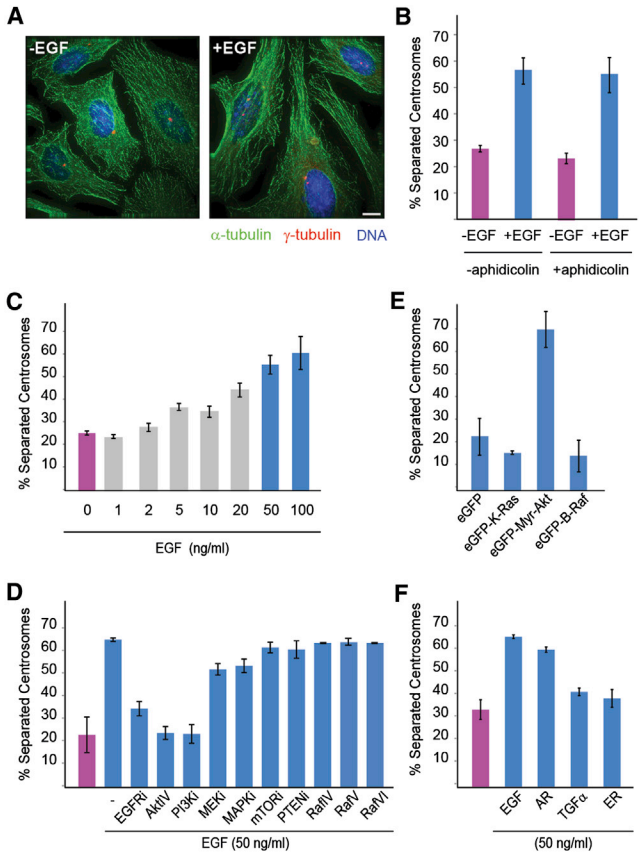

Figure 1. EGF Addition Induces Premature Centrosome Separation in S Phase

(A) HeLa cells were arrested in S phase and then treated with or without EGF (100 ng/ml) for 4 hr in the presence of aphidicolin. Cells were then fixed and stained for α- (green) and γ-tubulin (red). DNA is stained in blue. Scale bar represents 10 μm.

(B) Asynchronous (−aphidicolin) or S phase arrested (+aphidicolin) HeLa cells were incubated without (red bars) or with 50 ng/ml (blue bars) of EGF. The percentage of cells with separated centrosomes was scored. Results are from three independent experiments. n ≥ 300 cells were counted in each case. Data are presented as mean ± SD.

(C) HeLa cells arrested in S phase were treated with increasing concentrations of EGF and scored for the percentage of cells with separated centrosomes. Results are from two independent experiments. n ≥ 150 cells were counted in each case. Data are presented as mean ± SD.

(D) HeLa cells synchronized in S phase were kept untreated (red bar) or treated with 50 ng/ml EGF (blue bars) for 4 hr in the presence of the indicated inhibitors. Results are from three independent experiments. n ≥ 150 cells were counted in each case. Data are mean ± SD.

(E) HeLa cells were transfected with the indicated constructs and treated with 5 ng/ml of EGF. The percentage of cells with separated centrosomes was scored by indirect immunofluorescence. Results are from two independent experiments. n ≥ 50 cells were counted in each case. Data are presented as mean ± SD.

(F) HeLa cells were synchronized in S phase and kept untreated (red bar) or treated with indicated EGFR ligands (blue bars) for 4 hr. Epiregulin is depicted as ER and Amphiregulin is shown as AR. Results are from two independent experiments. n ≥ 150 cells were counted in each case. Data are mean ± SD. See also Figure S1.

for Eg5 in mitotic progression. Additionally, early centrosome separation promotes a rapid mitotic progression with fewer errors. The centrosomal response to EGFR signaling promotes proliferation and survival of cells. Importantly, cell types vary dramatically in their response to EGF making it possible to derive selective strategies to interfere with mitotic progression of cells with elevated EGFR signaling.

RESULTS

EGF Receptor Signaling Drives Premature Centrosome Separation via Akt Activation

To gain insights into the mechanisms of EGF-induced centrosome separation, we arrested HeLa cells in S phase and incubated them with EGF. As reported previously (Sherline and Mascardo, 1982), EGF addition rapidly induced centrosome separation in S phase (Figure 1A; Figure S1A and S1B available online). Importantly, EGF also triggered centrosome separation in asynchronous cells (Figure 1B, −aphidicolin), indicating that perturbation of DNA replication is not required for EGF-induced centrosome separation. Although 5 ng/ml EGF was sufficient to induce centrosome separation, maximal separation was achieved with 50 ng/ml EGF (Figure 1C).

EGF stimulates various signaling pathways through autophosphorylation of the EGF receptor (EGFR) (Normanno et al., 2006; Zwick et al., 1999). We exploited small molecule inhibitors of the major kinases of the EGFR signaling pathway to delineate the signaling cascade that ultimately promotes centrosome separation. Inhibition of EGFR signaling with the EGFR inhibitor Gefitinib blocked EGF-induced centrosome separation (Figure 1D; EGFRi). Importantly, inhibition of signaling downstream of EGFR with two different PI3K/Akt inhibitors (AktIV, PI3Ki), but not inhibitors against MEK kinase and downstream MAPK (MEKi, MAPKi), mTOR, PTEN phosphatase, or Raf kinase (RafIV, V, and VI) blocked EGF-induced centrosome separation (Figure 1D). Consistently, overexpression of myristoylated, active form of Akt (Myr-Akt) promoted centrosome separation whereas B-Raf and K-Ras did not (Figure 1E). Myr-Akt induced centrosome separation most efficiently when the cells were sensitized with 5 ng/ml EGF. We therefore conclude that EGF induces premature centrosome separation through activation of Akt of the EGFR signaling pathway.

Next, we stimulated the EGFR signaling by the addition of different ligands that are known to bind and activate the EGFR. Addition of TGFα and Epiregulin (ER) had little effect on centrosome separation whereas we observed an increased rate of centrosome separation in cells treated with Amphiregulin (AR) (Figure 1F). EGF family ligands trigger different biological outcomes by stimulating the same receptor (Citri and Yarden, 2006; Wilson et al., 2009). Our results indicate that the downstream signals activated by EGF or AR initiate premature centrosome separation.

EGF-Induced Centrosome Separation Requires the Mst2-Nek2A Pathway

Two distinct pathways contribute to centrosome separation during normal cell cycle progression. First, Nek2A initiates centrosome separation in G2 through phosphorylation of the linker proteins C-Nap1 and rootletin. This function of Nek2A is stimulated by two components of the Hippo pathway, Mst2 and hSav1, and by the Polo-like kinase Plk1 (Mardin et al., 2010, 2011). A second pathway relies on the kinesin Eg5, which

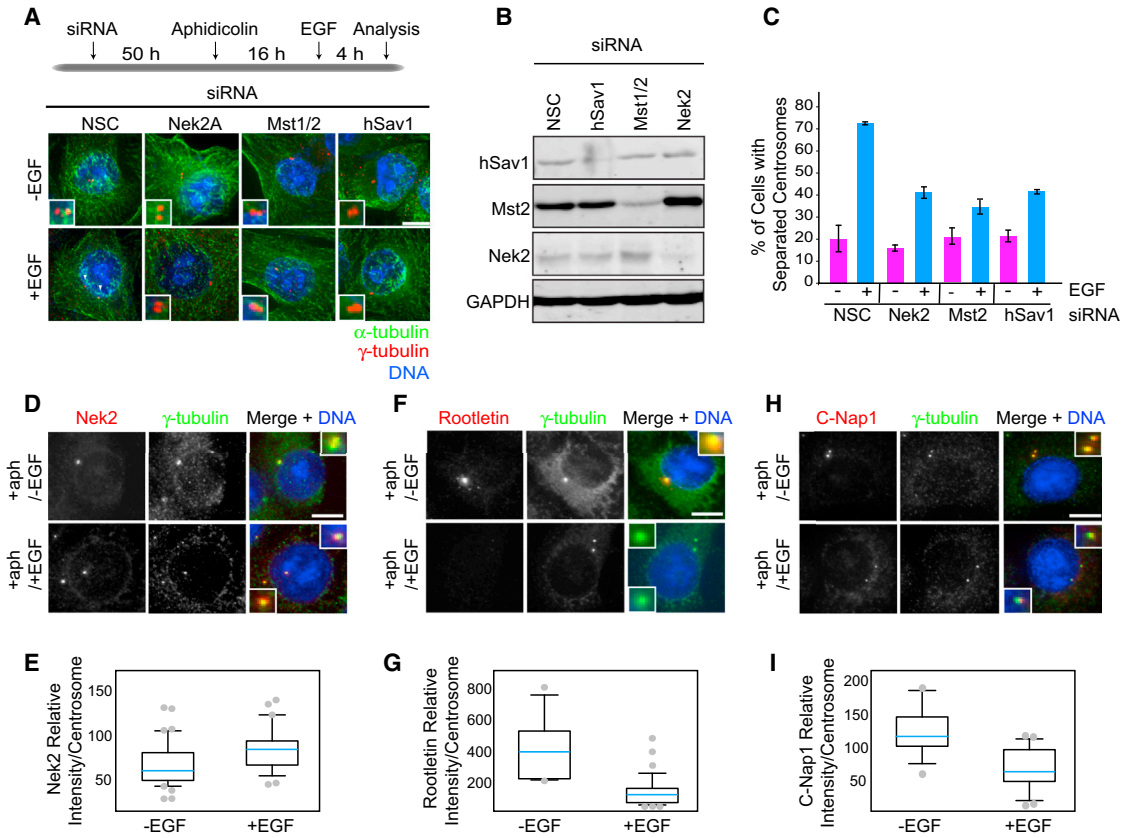

Figure 2. EGF Induces Centrosome Separation through the Mst2-hSav1-Nek2A Kinase Module

(A) HeLa cells were transfected with NSC (nonspecific control), Nek2, Mst1/2, or hSav1 siRNA oligos, arrested in S phase and either kept untreated or treated with 50 ng/ml EGF for four hours. Cells were then fixed and costained with α- and γ-tubulin antibodies. Scale bar represents 10 μm. Insets show the magnified centrosomes in each panel.

(B) Extracts of nonspecific control (NSC), Nek2, Mst1/2, or hSav1 siRNA-treated HeLa cells were analyzed by immunoblotting using GAPDH, hSav1, Mst1/2, and Nek2 antibodies.

(C) Quantification of the analysis in (A). Results are from three independent experiments. n ≥ 100 cells counted for each condition. Data are mean ± SD.

(D–I) HeLa cells were treated as in (A). Cells were then fixed and costained for γ-tubulin and Nek2 (D), rootletin (F), or C-Nap1 (H) antibodies. Scale bar represents 10 μm. The intensity of centrosomal Nek2 (E), rootletin (G), and C-Nap1 signals (I) in cells from (D), (F), and (H) were measured. The average background intensity was subtracted and the intensities were normalized to corresponding γ-tubulin signals. Results are from three independent experiments. n > 30 cells were analyzed for each condition. Box-and-whiskers plots: boxes show the upper and lower quartiles (25%–75%) with a line at the median, whiskers extend from the 10th to the 90th percentile and dots correspond to the outliers.

See also Figure S2.

can drive centrosome separation even in the absence of Nek2A (Mardin et al., 2010). We sought to determine the role of Nek2A- and Eg5-dependent pathways in EGF-induced premature centrosome separation. Depletion of Nek2A, hSav1 or Mst2 by siRNA significantly reduced the fraction of cells with separated centrosomes upon EGF addition (Figures 2A–2C). In contrast, inhibition of Eg5 with S-Trityl-L-Cysteine (STLC) (Skoufias et al., 2006) had no effect on EGF-induced centrosome separation (Figure S2A). Moreover, EGF-induced centrosome separation did not require the activity of the major mitotic kinases, including Plk1 (Figure S2A) and was independent of other components of the Hippo pathway (Figure S2B). These results suggest that EGF promotes centrosome separation by activating the Nek2A kinase pathway.

Interestingly, EGF-induced centrosome separation was not affected by global inhibition of translation or transcription (Figure S2A, CHX, ActD, and S2C). Moreover, the protein levels of Nek2A and Mst2 in S phase-arrested cells did not change upon cell stimulation with EGF (Figure S2D). Because accumulation of Nek2A at the centrosomes directly correlates with its local activity (Mardin et al., 2010), we reasoned that an enhancement in Nek2A recruitment to centrosomes might trigger EGF-induced centrosome separation. Indirect immunofluorescence of cells treated with EGF during S phase revealed a significant increase in centrosome-associated Nek2A (Figures 2D and 2E; $p < 0.006$). Consistently, the levels of Nek2A substrates at the centrosome, C-Nap1 and rootletin, were significantly reduced upon EGF stimulation (Figures 2F–2I; $p < 0.006$ and $p < 0.0001$ for C-Nap1 and rootletin, respectively). Together, these results indicate that the EGF-induced centrosome separation in S phase arises from stimulation of the Mst2-hSav1-Nek2A pathway, which leads to the accumulation of Nek2A at centrosomes where it promotes disassembly of the centrosomal linker.

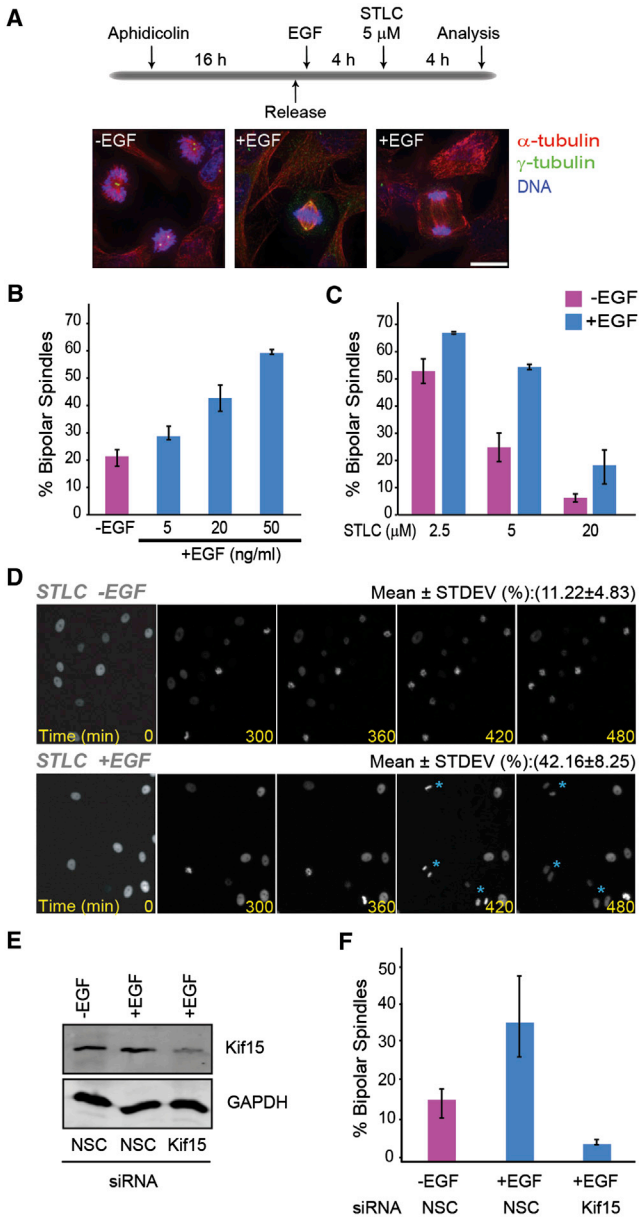

Figure 3. EGF Reduces the Requirement of Eg5 during Mitosis

(A) HeLa cells were arrested in S phase, released into G2 with or without EGF addition (50 ng/ml), and re-arrested in early mitosis by 5 μM STLC for 4 hr. Cells were then fixed and stained with α- and γ-tubulin antibodies. Scale bar represents 5 μm.

(B) Cells were treated as in (A) with 5 μM STLC and then incubated with the indicated EGF concentrations. Cells were analyzed for their ability to form bipolar spindles. Results are from three independent experiments. n > 100 cells were counted for each condition. Data are mean ± SD.

(C) Cells were treated with aphidicolin and with (blue bars) or without EGF (50 ng/ml) (red bars) as in (A) followed by incubation with the indicated STLC concentrations. Cells were then analyzed for their ability to form a bipolar spindle. Results are from three independent experiments. n > 100 cells counted for each condition. Data are mean ± SD.

(D) Still images taken from movies of HeLa cells stably expressing H2B-mCherry. Cells were first arrested in S phase, released into G2 with or without EGF (50 ng/ml) addition, and then imaged every 6 min in the presence of 5 μM STLC. The percentage of cells that completed mitosis is indicated above the panels. n > 50 cells analyzed for each condition. Asterisks indicate the dividing cells in the sample.

(E) Extracts of nonspecific control (NSC), or hKlp2/Kif15 siRNA-treated HeLa H2B-mCherry cells were analyzed by immunoblotting using GAPDH and hKlp2/Kif15 antibodies.

(F) HeLa H2B-mCherry cells were transfected with NSC or hKlp2/Kif15 siRNA oligos, arrested in S phase, released into G2 with or without EGF addition, and imaged every 6 min in the presence of 5 μM STLC. The cells were analyzed for their ability to form bipolar spindles. Data are mean ± SD.

See also Figures S3 and S4 and Movie S1.

Premature Centrosome Separation Promotes Eg5-Independent Bipolar Spindle Assembly

Upon disassembly of the centrosomal linker, Eg5 moves the centrosomes apart to establish the bipolar spindle (Bruinsma et al., 2012; Mardin et al., 2010; Mardin and Schiebel, 2012). We examined the impact of EGF stimulation on bipolar spindle assembly. Without additional EGF in the medium, inhibition of Eg5 with STLC prevented bipolar spindle assembly and blocked cell cycle progression in prometaphase (Figure 3A). Strikingly, however, stimulation of cells with EGF allowed cells to assemble bipolar spindles and progress through mitosis even in the presence of low Eg5 activity. The rate of progression through mitosis in the presence of Eg5 inhibition was positively correlated with the concentration of EGF (Figure 3B) and was observed even when STLC concentrations as high as 20 μM were used to block Eg5 activity (Figure 3C). To exclude that EGF affects the response of cells to STLC via upregulation of hKlp2/Kif15 or indirectly, we first established that EGF did not influence cellular Eg5 or hKlp2/Kif15 levels (Figure S2D). In addition, we confirmed that the inhibition of Eg5 with STLC was not affected by EGF stimulation judged by the antibody staining of Eg5 in mitotic cells, which relies on the direct correlation between Eg5 localization and activity (Mardin et al., 2011; Sawin and Mitchison, 1995) (Figure S3A). Moreover, when we depleted Eg5 by siRNA cells assembled bipolar spindles only in the presence of EGF (Figures S3B and S3C). These observations with fixed cells were confirmed by live cell imaging of HeLa cells stably expressing the histone H2B fused to mCherry as a chromatin marker (Figure 3D; Movie S1). Importantly, blocking centrosome separation by codepletion of Mst2 and Nek2 prior to EGF stimulation did not allow the cells to bypass the requirement of Eg5 upon EGF addition (Figures S4A and S4B). Together, these results indicate that the activation of the EGFR signaling and the induction of premature centrosome separation reduces the requirement for Eg5 during bipolar spindle assembly.

The ability to form bipolar spindles in cells with reduced Eg5 activity prompted us to investigate whether an alternative motor replaces Eg5 function in response to active EGFR signaling. The kinesin hKlp2/Kif15 appears to take over bipolar spindle formation when Eg5 activity is compromised (Tanenbaum et al., 2009; Vanneste et al., 2009). Analysis of cells in S phase with active EGFR signaling revealed that centrosome separation was independent of kinesin hKlp2/Kif15 as well as of dynein (Figure S4C). However, bipolar spindle assembly in EGF-stimulated cells in the presence of STLC was efficiently blocked by depletion of hKlp2/Kif15 (Figures 3E and 3F [live cell imaging] and S4D and S4E [time course experiment]). We conclude that hKlp2/Kif15 is required for Eg5-independent bipolar spindle assembly in EGF-treated cells.

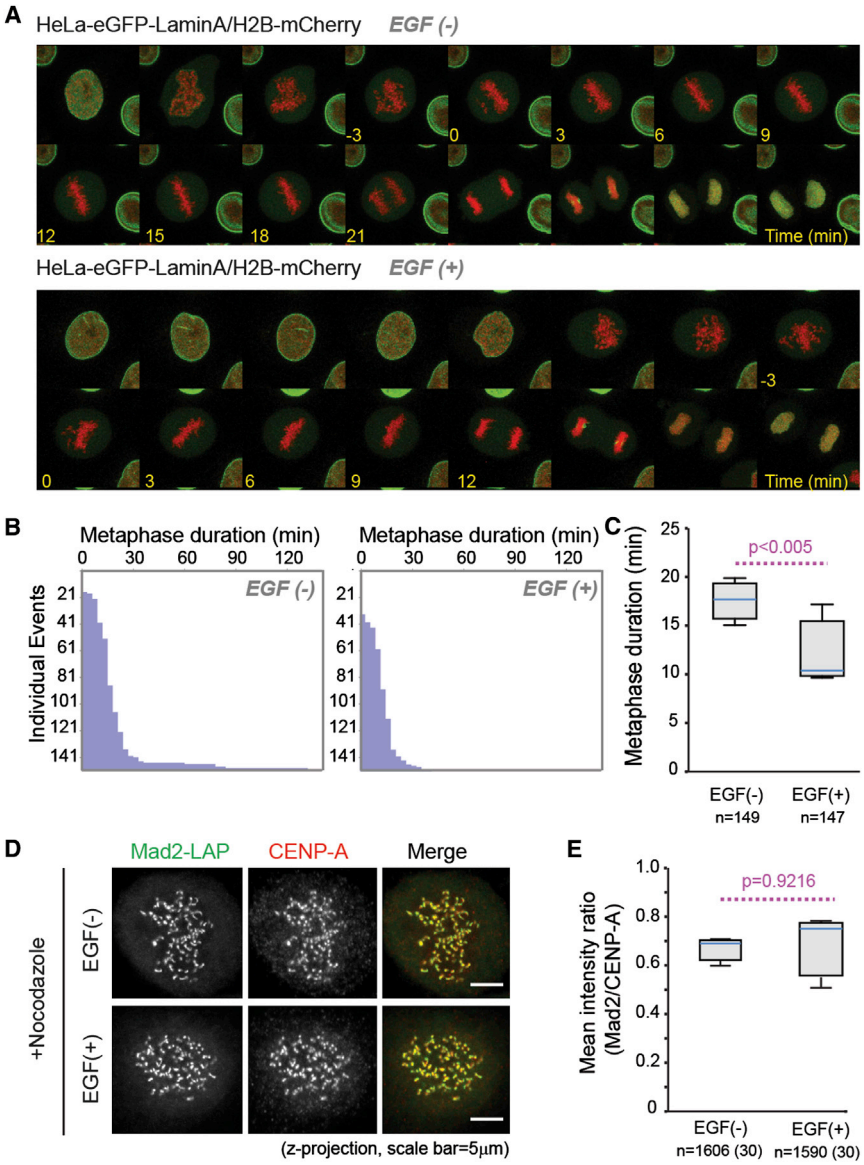

Figure 4. EGFR Signaling Accelerates Mitosis

(A) Still images from the movies of HeLa cells stably expressing eGFP-LaminA and H2B-mCherry with and without EGF addition following their release from S phase arrest. Images are collected with a time resolution of 3 min. Time spent during metaphase is indicated in minutes.

(B) Individual cell histories during metaphase progression. Each horizontal bar represents one cell. The records are sorted according to the metaphase progression rate. n = 147 and 149 events were analyzed for cells with (+EGF) and without (−EGF), respectively.

(C) Quantification of the events shown in (B). Metaphase progression in single cells was automatically measured after classification of cells by cell cognition. Box-and-whiskers plots: boxes show the upper and lower quartiles (25%–75%) with a line at the median, whiskers extend to minimum and maximum values.

(D) HeLa cells expressing Mad2-LAP and H2B-mCherry were incubated with or without EGF in the presence of nocodazole. Cells were fixed and stained with monoclonal Cenp-A antibodies. Scale bar represents 5 μm.

(E) Ratiometric analysis of the Mad2:Cenp-A signal intensities of cells in (D). Signal intensities on the kinetochores were analyzed automatically. Box-and-whiskers plots: boxes show the upper and lower quartiles (25%–75%) with a line at the median, whiskers extend to minimum and maximum values.

See also Figure S5 and Movie S2.

EGFR Signaling Accelerates Mitosis, Particularly during Metaphase

Next, we tested whether EGF-induced centrosome separation has any beneficial impact upon mitotic progression in an unperturbed cell division. We followed HeLa cells stably expressing EGFP-LaminA and H2B-mCherry (Mall et al., 2012) by live cell imaging together with and without EGF addition following their release from S phase arrest (Figure 4A). When centrosome separation was promoted in S phase by EGF, timing of metaphase was decreased on average by 8 min (Figures 4B and 4C; Movie S2) meaning that duration of metaphase was reduced by 44%. Interestingly, acceleration of mitosis in response to EGF correlated with its impact upon centrosome separation as codepletion of Mst2 and Nek2 neutralized the impact of EGF addition (Figures S5A and S5B; Movie S3).

Given that the EGF addition causes the cells to align their chromosomes faster on the metaphase plate, we asked whether the spindle assembly checkpoint (SAC) is affected in EGF-treated cells. HeLa cells expressing Mad2-LAP (Poser et al., 2008) were released from the aphidicolin block with or without EGF addition and arrested in prometaphase with nocodazole. Most kinetochores (labeled with CENP-A antibodies) colocalized with the SAC component Mad2. Ratiometric analysis of the Mad2/CENP-A intensities of over 1,500 kinetochores showed that Mad2 was equally recruited to kinetochores with or without EGF addition (Figures 4D and 4E) that suggests that the SAC is not affected by EGF (Chen et al., 1996; Waters et al., 1998). This notion is consistent with the observation that cells remained equally arrested in prometaphase when they are challenged by different concentrations of nocodazole together with or without EGF (Figure S5C).

EGFR Signaling Increases Fidelity of Chromosome Segregation in Genetically Unstable Cells

Our results suggest that EGF accelerates mitosis possibly due to premature separation of centrosomes. Previous studies have suggested an impact of the timing of centrosome separation on mitotic progression and fidelity (Indjeian and Murray, 2007; Kaseda et al., 2012; Silkworth et al., 2012). In order to test the effect of EGF-induced centrosome separation on mitotic fidelity,

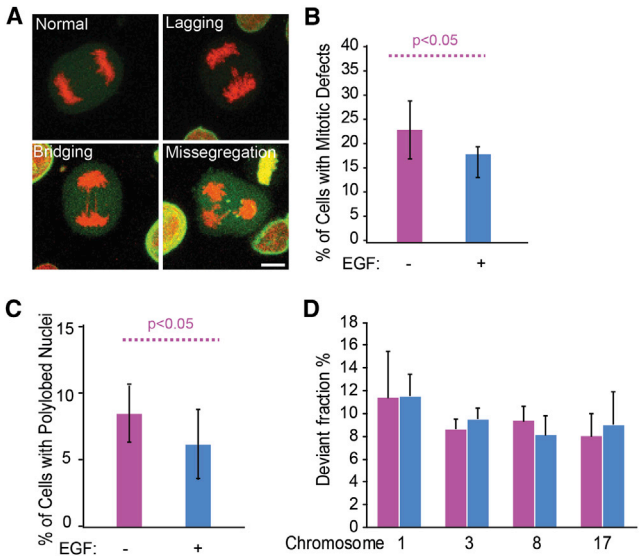

Figure 5. EGFR Signaling Increases Fidelity of Chromosome Segregation

(A) Representative images of different classes of mitotic defects that were analyzed from movies in Figure 4A. Scale bar represents 5 μm. See also Movie S3.

(B) Manual quantification of mitotic defects from movies of HeLa-eGFP-LaminA/H2B-mCherry cells that were treated with or without EGF (50 ng/ml). Movies of five independent experiments were analyzed. Data are mean ± SD.

(C) HeLa-eGFP-LaminA/H2B-mCherry cells were cultured in the presence or absence of EGF for 6 days. For the last division, they were imaged by high content screening microscopy and automatically scored for the formation of the polylobed nuclei. In total, 5,800 cells for untreated samples and 3,600 cells for EGF-treated samples were analyzed. Data are mean ± SD.

(D) HCT116 cells were incubated with (blue bars) or without (purple bars) EGF for 6 days. Cells were then fixed and analyzed by FISH with four different chromosome-specific centromere probes. Deviant fractions represent the percentages of the cells deviating from the modal number (two for HCT116 cells for all the four chromosomes analyzed). n > 800 for all measurements. Data are mean ± SD.

we first analyzed the rate of spontaneous mitotic errors from the movies shown in Figure 4A. Under our experimental conditions, ~20% of HeLa-eGFP-LaminA/H2B-mCherry cells showed various mitotic defects such as lagging chromosomes, chromosome bridges, and chromosome missegregation without EGF addition (Figures 5A and 5B). Addition of EGF significantly reduced these mitotic defects and increased the fidelity of mitosis (Figure 5B).

We reasoned that the decrease in mitotic errors by EGF should eventually lead to decreased genomic instability. In order to investigate this we incubated HeLa-eGFP-LaminA/H2B-mCherry cells for 6 days with and without EGF. During the last division we imaged these cells by high content screening microscopy and scored thousands of cells for the formation of polylobed nuclei indicative of mitotic exit with aberrant chromosome segregation (Neumann et al., 2010). A significant reduction of polylobed nuclei was observed in cells that were treated with EGF (Figure 5C). Thus, EGFR signaling in HeLa cells does not only accelerate mitosis, it also promotes the accuracy of chromosome segregation.

Using fluorescence in situ hybridization (FISH) we asked how cells with a stable chromosome set segregate the chromosomes in response to high levels of EGFR signaling. HCT116 cells have a stable chromosome set (Lengauer et al., 1997) and show intermediate sensitivity to EGF-induced centrosome separation (2-fold increase in S phase centrosome separation in response to EGF; Figure 6A). After culturing cells for 6 days with and without EGF, interphase FISH was used to analyze cells for the rates of whole chromosome missegregation (Figure 5D). Using four different chromosome-specific probes, we detected no significant difference in chromosome missegregation rates under these experimental conditions. In conclusion, EGFR signaling promotes the fidelity of chromosome segregation in genetically unstable cells and has little effect on chromosome stability in cells that are genetically stable.

The Impact of EGF on Centrosome Separation Depends on Basal EGFR Signaling

The timing of centrosome separation is highly variable between cell lines (McHedlishvili et al., 2012; Toso et al., 2009). To determine whether the activity of the EGFR signaling pathway accounts for this variation, we analyzed the degree of centrosome separation and its dependency on the EGFR signaling in several cancer cell lines of pancreatic (CAPAN-1 and AsPC-1), mammary (MCF-7), renal (ACHN), bone (U2OS), colorectal (HCT116), lung (NCI-H358 and NCI-H460), and cervical (HeLa) origins, and in two untransformed cell lines (RPE-1 [retina] and HPDE [pancreas]). We arrested all cells in S phase and determined the percentage of cells with separated centrosomes after incubation with 1 to 100 ng/ml EGF. CAPAN and AsPC-1 cells displayed particularly high levels of centrosome separation even without EGF addition (55%–60% for CAPAN-1 and 35%–40% for AsPC-1), which further increased in the presence of EGF (Figure 6A). HeLa cells showed moderate centrosome separation of ~20%–25% in S phase in the absence of EGF addition and responded well to EGF with ~60%–70% of cells displaying separated centrosomes. In contrast, the nontransformed RPE-1 and HPDE cells had particularly low levels of centrosome separation in S phase and both were refractory to high concentrations of EGF.

This result prompted us to investigate whether there is any correlation between the degree of centrosome separation and EGFR signaling. We selected four cell lines displaying the full spectrum of centrosome separation phenotypes (RPE-1, HeLa, AsPC-1, and CAPAN-1) for further studies. We found that CAPAN and AsPC-1 cells expressed particularly high levels of the EGF receptor, which correlated with the high levels of centrosome separation in S phase (Figures 6A and 6B). Moreover, we observed particularly high levels of centrosome-associated Nek2 in EGF-responsive cell lines in contrast to RPE-1 cells by quantitative immunofluorescence. EGF addition enhanced Nek2 recruitment to centrosomes in all cell lines. In RPE-1 cells this increase was moderate and remained below the levels of Nek2 in the other cell lines (Figure 6C). It is likely that the critical threshold that is needed to trigger centrosome splitting was not exceeded in RPE-1 cells.

We next asked if we could alter the level of centrosome separation in one of these cell lines by modifying the levels of EGFR signaling. We approached this question from two different

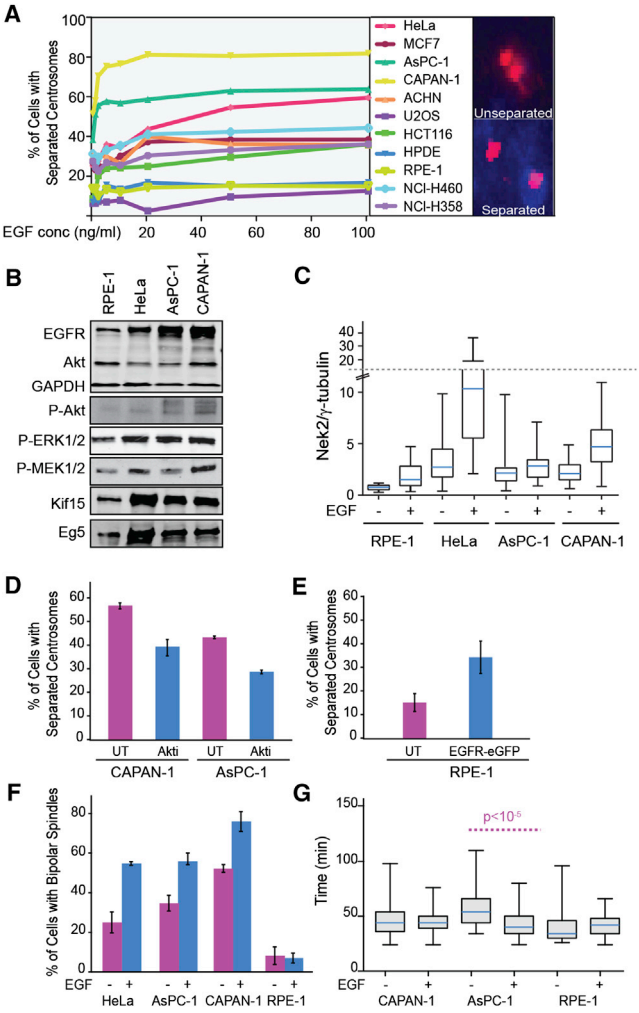

Figure 6. EGFR Signaling Induces Different Levels of Centrosome Separation

(A) All cells were arrested in S phase by aphidicolin and the frequency of centrosome separation was analyzed in the presence of increasing concentrations of EGF (1–100 ng/ml). n > 100 cells were counted for each condition. Examples of separated and unseparated centrosomes with γ-tubulin staining (red) are shown.

(B) Asynchronous RPE-1, HeLa, AsPC-1, and CAPAN-1 cells were induced with 50 ng/ml EGF. Cell extracts were analyzed after blotting with indicated antibodies.

(C) RPE-1, HeLa, AsPC-1, and CAPAN-1 cells were arrested in S phase, and then treated with or without EGF (50 ng/ml). Cells were stained with γ-tubulin and Nek2 antibodies and the centrosomal association of Nek2 was determined in relation to γ-tubulin. Box-and-whiskers plots: boxes show the upper and lower quartiles (25%–75%) with a line at the median, whiskers extend to minimum and maximum values.

(D) CAPAN-1 and AsPC-1 cells were treated with or without Akt inhibitor IV and arrested in S phase. Cells were then stained with γ-tubulin antibodies and scored for the number of cells with separated centrosomes. Data are mean ± SD.

(E) RPE-1 cells were transfected with EGFR-eGFP for 18 hr while being arrested in S phase by aphidicolin. Cells were then fixed and analyzed by indirect immunofluorescence. The percentage of cells with separated centrosomes was scored. Results are from three independent experiments. n ≥ 30 cells were counted in each case. Data are presented as mean ± SD.

(F) RPE-1, HeLa, AsPC-1, and CAPAN-1 cells were arrested in S phase, released into G2 with or without EGF addition (50 ng/ml), and treated with 5 μM STLC for 4 hr. Cells were then analyzed for their ability to form bipolar spindles. Results are from three independent experiments. n > 50 cells counted for each condition. Data are mean ± SD.

(G) Average time from chromosome condensation to anaphase (RPE-1 H2B-RFP) or cell rounding to chromosome segregation (AsPC-1 and CAPAN-1) was quantified for cells with and without EGF addition (50 ng/ml). Box-and-whiskers plots: boxes show the upper and lower quartiles (25%–75%) with a line at the median, whiskers extend to minimum and maximum values.

See also Figure S6.

perspectives. First, we inhibited downstream EGFR signaling by Akt inhibitor IV in AsPC-1 and CAPAN-1 cells that have high levels of basal centrosome separation. Interestingly, this treatment reduced centrosome separation in AsPC-1 and CAPAN-1 cells suggesting a direct involvement of high EGFR signaling in centrosome separation (Figure 6D). Second, we overexpressed EGFR in RPE-1 cells and found that the EGFR increased the percentage of S phase cells with separated centrosomes 2-fold further supporting a direct effect of high EGFR signaling on centrosome separation (Figure 6E). Taken together, the differences in centrosome separation efficiency between different cell lines are at least in part a reflection of the basal activity of the EGFR signaling pathway.

Our previous results suggested that the timing of centrosome separation might have an impact on the requirement of Eg5 for spindle assembly. For this reason, we analyzed mitotic progression of RPE-1, HeLa, AsPC-1, and CAPAN-1 cells that are released from S phase in the presence of 5 μM STLC together with or without addition of EGF (Figure 6F). Similar to our previous observations, addition of EGF promoted bipolar spindle formation in STLC-treated HeLa cells. In contrast, RPE-1 cells failed to form bipolar spindles even when treated with EGF. Importantly, 30%–50% of cells of the two pancreatic cell lines formed bipolar spindles in the presence of 5 μM STLC even without EGF addition. CAPAN-1 cells were more potent in bipolar spindle formation than AsPC-1 cells even without addition of EGF. This is consistent with the high level of EGFR expression in CAPAN-1 cells (Figure 6B) and the more frequent separation of centrosomes in S phase (Figure 6A) compared to AsPC-1 cells. Thus, the level of centrosome separation in S phase determines the requirement of Eg5 function for spindle formation.

We assessed the impact of EGF stimulation on mitotic progression in other cell lines. In synchronized RPE-1 H2B-mRFP cells we found no statistically significant difference in the timing of mitotic progression with or without EGF (Figure 6G). EGF addition to CAPAN-1 cells did not accelerate mitotic progression (from cell rounding to chromosome segregation), in line with their high level of basal centrosome separation in S phase cells prior to EGF addition. In contrast, mitotic progression of AsPC-1 cells was accelerated by 10 min in response to EGF (Figure 6G). This value is consistent with the degree of centrosome separation in AsPC-1 cells following EGF stimulation. Together, these data suggest that early centrosome separation by EGF facilitates spindle assembly.

Cell Proliferation in Response to Changes in EGFR Signaling and Eg5 Inhibition

The experiments described above raised the possibility that the level of EGFR signaling might influence the overall response of

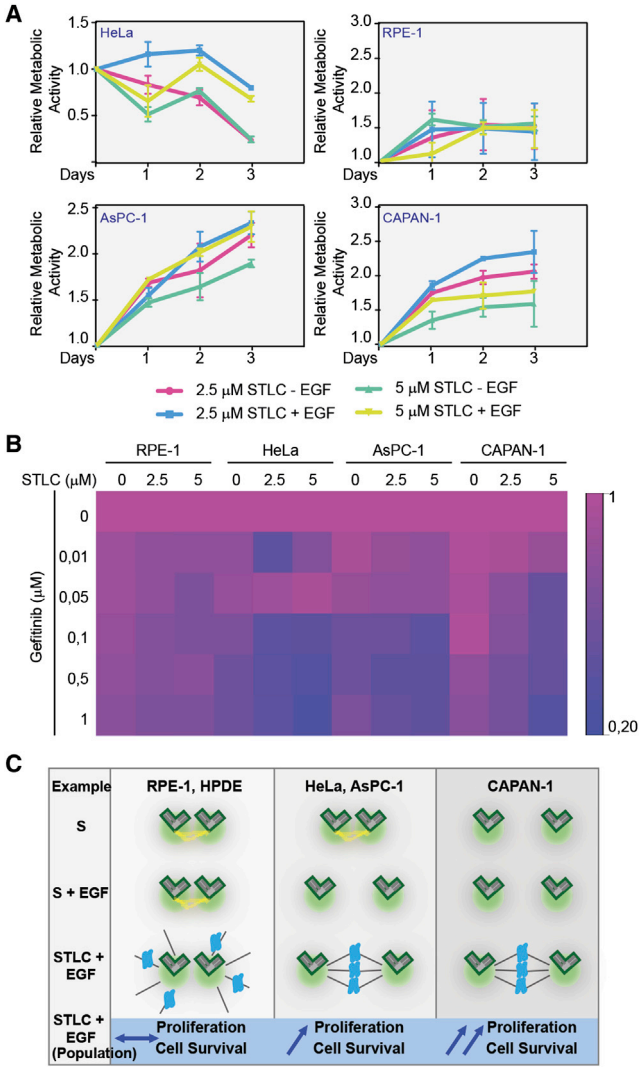

Figure 7. The Rates of Cell Proliferation and Survival in Cancer Cells Vary in Response to Changes in EGFR Signaling and Eg5 Inhibition

(A) RPE-1, HeLa, AsPC-1, and CAPAN-1 cells were treated with or without EGF (+/−) and incubated in the presence of STLC (2.5 or 5 μM) for 3 days. The metabolic activity of the cells was analyzed by the MTT assay and is presented relative to the activity at the start of the experiment in each case. The results are from three independent experiments. Data are mean ± SD.

(B) RPE-1, HeLa, AsPC-1, and CAPAN-1 cells were treated with EGFR kinase inhibitor Gefitinib (0 to 1 μM) and the Eg5 inhibitor STLC (0, 2.5, or 5 μM) for 3 days. The metabolic activity of the cells was analyzed by the MTT assay and is normalized relative to the activity of untreated cells. Heat maps are generated with GiTools software. For individual graphs see Figure S6C.

(C) EGF induces centrosome separation during S phase through the Akt branch of the signaling pathway. This leads to increased accumulation of Nek2A at the centrosomes resulting in premature resolution of the centrosome linker. During mitosis, this premature centrosome separation reduces the requirement for Eg5 in bipolar spindle formation but renders mitosis reliant upon the alternative motor hKlp2/Kif15. Different cell types respond differently to EGF addition at both single-cell and population level. See Discussion for details.

cells to Eg5 inhibition. To address this, we followed cells for 3 days in the presence of STLC (2.5 or 5 μM) with or without EGF treatment. Using an MTT assay to monitor metabolic activity of the cells, we found that STLC reduced the viability of HeLa cells over time; however, this inhibitory impact was rescued by EGF addition. In contrast, EGF had no effect on viability in response to STLC in RPE-1 cells. It is noteworthy that the EGF nonresponding HPDE-1 cells (Figure 6A), which have the same pancreatic origin as AsPC-1 and CAPAN-1 cells also showed no change in viability during these measurements (data not shown). In contrast, both AsPC-1 and CAPAN-1 cells increase their metabolic activity over time even in the presence of STLC. Importantly, this robust growth was further stimulated by EGF addition (Figure 7A).

We confirmed these observations by an independent assay that could simultaneously monitor cell proliferation and viability (Guava Via Count) by using a mixture of two DNA binding dyes: a membrane-permeable dye that stains all nucleated cells and a membrane-impermeable dye that only stains damaged cells thus giving a measure of the number of dying cells within a culture (Figures S6A and S6B). Decrease in viability of HeLa cells in response to STLC was suppressed by EGF addition. RPE-1 cells showed no response to EGF stimulation in terms of viability or proliferation, whereas both viability and proliferation were increased by EGF addition to AsPC-1 cells. These data support our previous observations that STLC has distinct impacts on cell fate in different cell lines in a manner that reflects the response of each cell line to EGF stimulation.

We reasoned that if EGF addition allows some cells to proliferate with very low Eg5 activity, repressing the EGFR pathway should sensitize these cells to Eg5 inhibition. In order to test this idea, we measured the response of cell lines to the combination of Eg5 and EGFR inhibition. For this we used the EGFR kinase inhibitor Gefitinib and the Eg5 inhibitor STLC, titrated the concentration of both drugs and generated heat maps based on the survival rate of the cells (Perez-Llamas and Lopez-Bigas, 2011) (Figures 7B and S6C). RPE-1 cells were not synergistically affected by the combination of Eg5 and EGFR kinase inhibition (Figure 7B). However, most pronounced in CAPAN-1 cells, neither Eg5 nor EGFR kinase inhibition alone caused a strong inhibition of metabolic activity, but a combination of both strikingly reduced the survival rate of these cells (Figure 7B). We observed a dose-dependent decrease in the survival of the cells, which suggests that the activity of the EGFR signaling in context of centrosome separation is critical for their response to Eg5 inhibition.

DISCUSSION

In this study, we demonstrate that stimulation of the EGFR signaling pathway by EGF induces premature centrosome separation in S phase through the activation of the Mst2-hSav1-Nek2A module that targets Nek2A kinase to the centrosomes. A direct consequence of our findings is that cells with high EGFR activity bypass the requirement of Eg5 for mitosis. This has important implications for cancer therapy because cancer cells with high EGFR signaling are more susceptible to combinatorial inhibition of EGFR and Eg5.

Control of Centrosome Separation by the EGFR Signaling Pathway

EGFR belongs to the ErbB family of receptor tyrosine kinases and is frequently upregulated in cancer cells (Avraham and Yarden, 2011; Klein and Levitzki, 2009). Although many complex interactions exist within this signaling pathway (Citri and Yarden, 2006), we found that the Akt branch is required for EGF-induced centrosome separation. In contrast, inhibitors against the lipid phosphatase PTEN, Raf kinase, MEK kinases, and the MAPK, or the growth controlling mTOR kinase had no effect on centrosome separation in S phase.

The PI3K/Akt pathway is deregulated in many tumors due to frequent mutations found in different components of the pathway (Altomare and Testa, 2005; Testa and Tsichlis, 2005). Presently, it is unclear whether Akt impacts directly on centrosome separation; however, Akt can directly phosphorylate Mst2 in serum-starved cells. In this context Akt phosphorylation inhibits Mst2 activity (Romano et al., 2010). Addition of EGF could also change the affinity of Mst2 for binding partners thus directly or indirectly promoting the association of Mst2 and Nek2.

Why do the cells need to control the timing of centrosome separation? Here we present evidence that the induction of premature centrosome separation affects the way mitosis is executed. First, addition of EGF and separation of the centrosomes in S phase considerably reduced the duration of mitosis particularly during metaphase alignment. This was not due to abrogation of SAC function because the Mad2:CENP-A ratio (Chen et al., 1996; Waters et al., 1998) was unaltered by EGF addition and cells responded equally to nocodazole with or without EGF. Most likely in cells that separate centrosomes before nuclear envelope breakdown, opposing kinetochores are captured faster by microtubules facilitating amphitelic attachments. Consistent with this, it was recently reported that HeLa cells that have separated centrosomes before nuclear envelope breakdown execute mitosis faster than cells with unseparated centrosomes (Kaseda et al., 2012). In addition, the configuration of chromosomes around the centrosomes during prometaphase promotes the formation of amphitelic attachments by exposing kinetochores to the centrosomally nucleated microtubules (Magidson et al., 2011). Similarly, we propose that positioning the centrosomes on the opposite sides of the nucleus prior to mitotic entry facilitates the formation of the bipolar spindle.

Second, HeLa cells treated with EGF executed mitosis more accurately than cells without EGF. This increase in precision is most likely a reflection of the more efficient spindle assembly pathway when centrosomes are separated ahead of nuclear envelope breakdown. However, in genetically stable HCT116 cells, EGFR signaling had no detectable influence on chromosome segregation fidelity. Thus, EGF signaling probably only shows its chromosome stabilizing function when the spindle apparatus is defective. Therefore, EGFR signaling will have benefits for chromosome segregation when mutations or unfavorable growth conditions such as downregulation of motor proteins or drug treatment favors chromosome missegregation.

During early tumorigenesis, some mutations may allow cells to overcome mitotic blocks giving cells a growth advantage. One example is the bypass of Eg5 motor activity for mitosis by the upregulation of EGFR. Recently, it was demonstrated that overexpression of hKlp2/Kif15 can bypass the requirement for Eg5 motor activity (Raaijmakers et al., 2012). Similarly, dissolution of the centrosomal linker ahead of nuclear envelope breakdown by EGF bypasses the need of Eg5 and hKlp2/Kif15 motor activity becomes sufficient to drive chromosome segregation. This is either because Eg5 motor activity is no longer required for separation of the centrosomal linker or the prometaphase spindle assembly pathway has less force requirement, which makes hKlp2/Kif15 sufficient to drive spindle assembly.

EGFR Activity Determines the Timing of Centrosome Separation and the Manner of Mitotic Progression in Cell Lines

While examining the fate of cells with different responses to EGF, we found that EGF addition induced centrosome separation only in a subset of cell lines. We detected a direct correlation between the degree of S phase centrosome separation and the requirement for Eg5 for bipolar spindle formation and responsiveness to EGF. We also observed a clear correlation between the expression of EGFR in cells and the levels of centrosome separation. Interestingly, overexpression of EGFR in RPE-1 cells triggered S phase separation of centrosomes even without addition of EGF. High basal levels of EGFR signaling therefore might account for the ability of some cell lines to separate centrosomes in S phase with low EGF concentrations.

On the basis of our observations, we partitioned the EGF response of cells into three categories (Figure 7C). The first group (e.g., RPE-1, HPDE) responded poorly to EGF and did not separate their centrosomes in S phase. These cells could not overcome Eg5 inhibition and EGF addition provided no advantage during mitosis. The second group responded well to EGF (e.g., HeLa and AsPC-1) and separated their centrosomes in S phase. Consistently, EGF addition allowed these cells to progress through mitosis despite Eg5 inhibition and provided a long-term advantage in proliferation and viability. The third group (e.g., CAPAN-1) had particularly high basal levels of centrosome separation in S phase. Therefore, addition of EGF to these cells had very little impact on centrosome separation. Yet these cells were able to progress through mitosis even in the absence of EGF and presence of 5 μM STLC. We therefore propose that targeting mitosis requires an understanding of the EGF response of a particular cell type not only in the context of G1/S transition but also mitotic progression.

Implications for Novel Combination Approaches to Cancer Therapy

Great efforts have been put into the discovery of drugs that target mitosis to arrest cell cycle progression and induce mitotic catastrophe in cancer cells while causing minimal cytotoxicity to normal dividing cells (Garnett et al., 2012). Spindle poisons such as paclitaxel are commonly used as cancer therapeutics (Risinger et al., 2009). By interfering with microtubule dynamics, paclitaxel induces mitotic arrest and apoptosis; however, the reliance of many nonmitotic processes, such as intracellular transport in the CNS, upon microtubules means that global targeting of microtubules has significant side effects and consequent toxicity issues. Targeting the kinesin Eg5, which is required for the formation of a bipolar spindle (Sawin et al.,

1992; Whitehead and Rattner, 1998), has therefore been a promising alternative to generate drugs that interfere with the microtubule-related aspects of cell division while having no impact upon nondividing tissues. However, this approach has displayed limited benefits in clinical trials due to nonspecific effects of high dose Eg5 inhibition (Gartner et al., 2005; Leizerman et al., 2004; Skoufias et al., 2006). Similarly, with the clear exception of female lung cancer, EGFR inhibitors as single therapeutic agents have not proven very efficient for selective elimination of tumor cells. In this study, we evaluated how activation of the EGFR signaling pathway is critical for the execution of mitosis and how it is differentially regulated in different cancer cell lines, thus proposing an alternative way to combine targets in cancer therapy. For this reason, multitargeted approaches based upon the level of inherent EGF signaling within a particular tumor type might be more attractive.

EXPERIMENTAL PROCEDURES

An extended version of the experimental procedures can be found in the Supplemental Experimental Procedures.

Cell Lines and Treatments

The HeLa Kyoto cell line expressing H2B-mCherry and EGFP-LaminA were provided by Iain W. Mattaj (EMBL, Heidelberg, Germany) (Mall et al., 2012). The HeLa Kyoto cell line expressing mMad2-LAP BAC was provided by Anthony A. Hyman (MPI, Dresden, Germany) (Poser et al., 2008). H2B-mCherry was transfected into HeLa cells expressing mMad2-LAP BAC with Fugene 6 (Roche) according to the instructions of the manufacturer. A clone stably expressing H2B-mCherry was isolated by selection with 0.5 μg/ml Puromycin (Calbiochem), HeLa WT, U2OS, ACHN, and MCF7 cells were maintained in DMEM medium. hTERT RPE-1 and RPE-1-H2B-mRFP cells were grown in DMEM F-12 medium, HCT116 cells in McCoy and CAPAN-1, AsPC-1 cells were grown in IMDM cells, and NCI358 and NCI460 cells in RPMI medium supplemented with heat inactivated 10% fetal bovine serum and 2 mM glutamine. HPDE cells were maintained in Keratinocyte SFM medium supplemented with at 37°C in a humidified atmosphere with 5% CO_2. For specific drug treatments, see Supplemental Experimental Procedures.

Imaging

Imaging on most indirect immunofluorescence samples was performed at 25°C on a DeltaVision RT system (Applied Precision) with an Olympus IX71 microscope equipped with FITC, TRITC and Cy5 filters (Chroma Technology), a plan-Apo 100× NA 1.4 and 60× NA 1.4 oil immersion objective (Olympus), a CoolSNAP HQ camera (Photometrics), a temperature controller (Precision Control), and Softworx software (Applied Precision).

For live cell imaging experiments shown in Figures 3D, 6G, and S5A, cells were seeded on Hi-Q4 culture dish (Nikon). Experiments were performed either on an Olympus IX81 microscope equipped with GFP and mCherry filters, a UPLSAPO 20×/0.75 Air objective, a Hamamatsu ORCA-R2 camera and temperature controller or on a Biostation system (Nikon) equipped with GFP and mCherry filters, 20× 0.5 NA and 40× 0.8 NA air objectives and DS-2MBWc camera. For the experiments shown in Figures 3D, images are acquired every 6 min and the prometaphase arrested cells were scored versus the cells that go through mitosis. For experiments shown in Figures 6G and S5A, images were acquired every 2 min, and the timing from the nuclear envelope breakdown to chromosome segregation was determined and plotted.

For the live cell imaging experiments shown in Figures 4, 5A, and 5B, the cells were imaged with the Zen 2010 Software on a Zeiss 780 confocal microscope with a 63× PlanApochromat oil objective, NA 1.4 (Carl Zeiss) and an in-house temperature controller. We used 6 z stacks with 2.65 μm intervals for each position. Images were acquired with 3 min time resolution. For experiments shown in Figure S5C, images were acquired every 5 min.

For the live cell imaging experiments demonstrated in Figure 5C, images were acquired with an automated epifluorescence microscope (IX-81; Olympus) equipped with Plan10×, NA 0.4; Olympus objective, GFP and mCherry filters and a ScanR software. An image-based autofocusing routine was used to focus on the maximum number of interphase cells (scoring size, intensity, contrast) in a field of view. The focus z coordinates of the positions were saved during the first round of imaging and applied to the other time points.

Fluorescence Intensity Measurements

ImageJ (http://rsb.info.nih.gov/ij) was used to define an area around the centrosome and near the centrosome (background), and to measure the mean fluorescence intensity. Unsplit centrosomes were measured together, whereas split centrosomes were measured separately. Average of background intensities were subtracted from measurements in each channel. Signal intensity of unsplit pairs was divided by 2 to get the average intensity at each centrosome. Signal intensities were corrected for corresponding γ-tubulin signals. In order to measure Nek2 intensity from different cell lines, images from one data set were acquired at the same day and exposure times were set equal between different samples. To measure distances between centrosomes, two poles were identified (according to γ-tubulin or centrin signals) from raw data and distance was determined by ImageJ. The centrosomes were considered as "separated" when the distance between the two poles was >2 μm.

Quantitative Immunofluorescence

For Mad2 localization studies that is shown in Figures 4D and 4E we used a cell line expressing H2B-mCherry and the mMad2 tagged with a modified version of the localization and affinity purification (LAP)-tag (Cheeseman and Desai, 2005) at its last exon, integrated in a bacterial artificial chromosome (BAC) (mMad2-LAP BAC) (Poser et al., 2008). Images of HeLa cells expressing H2B-mCherry and mMad2-LAP BAC were acquired on a Zeiss LSM780 confocal microscope with a 63× 1.4 NA oil objective (Carl Zeiss).

To measure mMad2 expression levels at kinetochore in 3D images, the nuclear shape after segmentation of the H2B-mCherry channel created a nuclear mask in which mMad2-LAP and anti-CENP-A mean intensity were measured. The overlapped CENP-A signals in 9 pixels circles were automatically excluded from the measurement. To correct for intensity variability of mMad2-LAP, we normalized mMAd2-LAP signal to the kinetochore signal of the CENP-A antibody. Segmentation and intensity measurements were carried out automatically by an in-house developed Fiji routine.

Automated Quantitative Phenotypic Analysis

Automated quantitative analysis of dividing H2B-mCherry and eGFP-laminA expressing cells was used to monitor for mitotic progression in single cells. For this, nuclei were detected in the H2B-mCherry channel and classified as previously described (Held et al., 2010; Walter et al., 2010). For classification, we defined nine morphological classes: interphase, prophase, prometaphase, metaphase, early anaphase, late anaphase, telophase, cell death, and polylobed nuclei. The training set contained 946 manually labeled nuclei, which were detected with an overall accuracy of more than 90.0%. Cells were tracked with a constrained nearest-neighbor tracking procedure, and mitotic onset was detected as interphase–prophase or interphase–prometaphase transition. To reduce the effect of classification errors on phase length measurements, classification results were corrected with hidden Markov models (Held et al., 2010). Triplicates with each at least 40 mitotic events per condition were analyzed. For each replicate, metaphase duration was automatically measured.

Cell Proliferation and Growth Assays

The MTT assay was used to quantify cytotoxicity. For the growth and viability tests, cells were analyzed using a small desktop Guava Personal Cytometer with Guava ViaCount software (Milipore). Viable populations were gated based on forward and side scatters.

SUPPLEMENTAL INFORMATION

Supplemental Information includes six figures, three movies, and Supplemental Experimental Procedures and can be found with this article online at http://dx.doi.org/10.1016/j.devcel.2013.03.012.

ACKNOWLEDGMENTS

We thank Stefanie Heinze for excellent technical support. We also thank J. Bulkescher for the help with High Content Screening microscopy. Dr. O. Sahin is acknowledged for the gift of EGFR and MEK kinase inhibitors, Dr. T. Mayer for siRNA oligonucleotides directed against hKlp2/Kif15, Drs. I. Vernos and R. Medema for antibodies against hKlp2/Kif15, Dr. C. Pritchard for lung cancer cell lines, and Dr. M. Martins for the myr-Akt construct. We thank Y. Zhang and Dr. N. Giese for their generous help in MTT and Guava assays and F.G. Agircan and B. Cerikan for help in tissue culture. We thank Drs. I. Hagan and A. Khmelinskii for critical comments to the manuscript. We are grateful to Dr. J.O. Korbel for his support during the revision process. This work was supported by financial support of the SFB1036. A.M.F. acknowledges support from the Association of International Cancer Research (AICR), the Wellcome Trust, and Cancer Research UK.

Received: August 17, 2012
Revised: January 31, 2013
Accepted: March 18, 2013
Published: May 2, 2013

REFERENCES

Altomare, D.A., and Testa, J.R. (2005). Perturbations of the AKT signaling pathway in human cancer. Oncogene *24*, 7455–7464.

Avraham, R., and Yarden, Y. (2011). Feedback regulation of EGFR signalling: decision making by early and delayed loops. Nat. Rev. Mol. Cell Biol. *12*, 104–117.

Bruinsma, W., Raaijmakers, J.A., and Medema, R.H. (2012). Switching Polo-like kinase-1 on and off in time and space. Trends Biochem. Sci. *37*, 534–542.

Cheeseman, I.M., and Desai, A. (2005). A combined approach for the localization and tandem affinity purification of protein complexes from metazoans. Sci. STKE *2005*, pl1.

Chen, R.H., Waters, J.C., Salmon, E.D., and Murray, A.W. (1996). Association of spindle assembly checkpoint component XMAD2 with unattached kinetochores. Science *274*, 242–246.

Citri, A., and Yarden, Y. (2006). EGF-ERBB signalling: towards the systems level. Nat. Rev. Mol. Cell Biol. *7*, 505–516.

Garnett, M.J., Edelman, E.J., Heidorn, S.J., Greenman, C.D., Dastur, A., Lau, K.W., Greninger, P., Thompson, I.R., Luo, X., Soares, J., et al. (2012). Systematic identification of genomic markers of drug sensitivity in cancer cells. Nature *483*, 570–575.

Gartner, M., Sunder-Plassmann, N., Seiler, J., Utz, M., Vernos, I., Surrey, T., and Giannis, A. (2005). Development and biological evaluation of potent and specific inhibitors of mitotic Kinesin Eg5. ChemBioChem *6*, 1173–1177.

Hackel, P.O., Zwick, E., Prenzel, N., and Ullrich, A. (1999). Epidermal growth factor receptors: critical mediators of multiple receptor pathways. Curr. Opin. Cell Biol. *11*, 184–189.

Held, M., Schmitz, M.H., Fischer, B., Walter, T., Neumann, B., Olma, M.H., Peter, M., Ellenberg, J., and Gerlich, D.W. (2010). CellCognition: time-resolved phenotype annotation in high-throughput live cell imaging. Nat. Methods *7*, 747–754.

Hynes, N.E., and MacDonald, G. (2009). ErbB receptors and signaling pathways in cancer. Curr. Opin. Cell Biol. *21*, 177–184.

Indjeian, V.B., and Murray, A.W. (2007). Budding yeast mitotic chromosomes have an intrinsic bias to biorient on the spindle. Curr. Biol. *17*, 1837–1846.

Kapoor, T.M., Mayer, T.U., Coughlin, M.L., and Mitchison, T.J. (2000). Probing spindle assembly mechanisms with monastrol, a small molecule inhibitor of the mitotic kinesin, Eg5. J. Cell Biol. *150*, 975–988.

Kaseda, K., McAinsh, A.D., and Cross, R.A. (2012). Dual pathway spindle assembly increases both the speed and the fidelity of mitosis. Biol. Open *1*, 12–18.

Klein, S., and Levitzki, A. (2009). Targeting the EGFR and the PKB pathway in cancer. Curr. Opin. Cell Biol. *21*, 185–193.

Leizerman, I., Avunie-Masala, R., Elkabets, M., Fich, A., and Gheber, L. (2004). Differential effects of monastrol in two human cell lines. Cell. Mol. Life Sci. *61*, 2060–2070.

Lengauer, C., Kinzler, K.W., and Vogelstein, B. (1997). Genetic instability in colorectal cancers. Nature *386*, 623–627.

Magidson, V., O'Connell, C.B., Lončarek, J., Paul, R., Mogilner, A., and Khodjakov, A. (2011). The spatial arrangement of chromosomes during prometaphase facilitates spindle assembly. Cell *146*, 555–567.

Mall, M., Walter, T., Gorjánácz, M., Davidson, I.F., Nga Ly-Hartig, T.B., Ellenberg, J., and Mattaj, I.W. (2012). Mitotic lamin disassembly is triggered by lipid-mediated signaling. J. Cell Biol. *198*, 981–990.

Mardin, B.R., and Schiebel, E. (2012). Breaking the ties that bind: new advances in centrosome biology. J. Cell Biol. *197*, 11–18.

Mardin, B.R., Lange, C., Baxter, J.E., Hardy, T., Scholz, S.R., Fry, A.M., and Schiebel, E. (2010). Components of the Hippo pathway cooperate with Nek2 kinase to regulate centrosome disjunction. Nat. Cell Biol. *12*, 1166–1176.

Mardin, B.R., Agircan, F.G., Lange, C., and Schiebel, E. (2011). Plk1 controls the Nek2A-PP1γ antagonism in centrosome disjunction. Curr. Biol. *21*, 1145–1151.

Mayer, T.U., Kapoor, T.M., Haggarty, S.J., King, R.W., Schreiber, S.L., and Mitchison, T.J. (1999). Small molecule inhibitor of mitotic spindle bipolarity identified in a phenotype-based screen. Science *286*, 971–974.

McHedlishvili, N., Wieser, S., Holtackers, R., Mouysset, J., Belwal, M., Amaro, A.C., and Meraldi, P. (2012). Kinetochores accelerate centrosome separation to ensure faithful chromosome segregation. J. Cell Sci. *125*, 906–918.

Neumann, B., Walter, T., Hériché, J.K., Bulkescher, J., Erfle, H., Conrad, C., Rogers, P., Poser, I., Held, M., Liebel, U., et al. (2010). Phenotypic profiling of the human genome by time-lapse microscopy reveals cell division genes. Nature *464*, 721–727.

Normanno, N., De Luca, A., Bianco, C., Strizzi, L., Mancino, M., Maiello, M.R., Carotenuto, A., De Feo, G., Caponigro, F., and Salomon, D.S. (2006). Epidermal growth factor receptor (EGFR) signaling in cancer. Gene *366*, 2–16.

Perez-Llamas, C., and Lopez-Bigas, N. (2011). Gitools: analysis and visualisation of genomic data using interactive heat-maps. PLoS ONE *6*, e19541.

Poser, I., Sarov, M., Hutchins, J.R., Hériché, J.K., Toyoda, Y., Pozniakovsky, A., Weigl, D., Nitzsche, A., Hegemann, B., Bird, A.W., et al. (2008). BAC TransgeneOmics: a high-throughput method for exploration of protein function in mammals. Nat. Methods *5*, 409–415.

Raaijmakers, J.A., van Heesbeen, R.G., Meaders, J.L., Geers, E.F., Fernandez-Garcia, B., Medema, R.H., and Tanenbaum, M.E. (2012). Nuclear envelope-associated dynein drives prophase centrosome separation and enables Eg5-independent bipolar spindle formation. EMBO J. *31*, 4179–4190.

Risinger, A.L., Giles, F.J., and Mooberry, S.L. (2009). Microtubule dynamics as a target in oncology. Cancer Treat. Rev. *35*, 255–261.

Romano, D., Matallanas, D., Weitsman, G., Preisinger, C., Ng, T., and Kolch, W. (2010). Proapoptotic kinase MST2 coordinates signaling crosstalk between RASSF1A, Raf-1, and Akt. Cancer Res. *70*, 1195–1203.

Sawin, K.E., and Mitchison, T.J. (1995). Mutations in the kinesin-like protein Eg5 disrupting localization to the mitotic spindle. Proc. Natl. Acad. Sci. USA *92*, 4289–4293.

Sawin, K.E., LeGuellec, K., Philippe, M., and Mitchison, T.J. (1992). Mitotic spindle organization by a plus-end-directed microtubule motor. Nature *359*, 540–543.

Sherline, P., and Mascardo, R.N. (1982). Epidermal growth factor induces rapid centrosomal separation in HeLa and 3T3 cells. J. Cell Biol. *93*, 507–512.

Silkworth, W.T., Nardi, I.K., Paul, R., Mogilner, A., and Cimini, D. (2012). Timing of centrosome separation is important for accurate chromosome segregation. Mol. Biol. Cell *23*, 401–411.

Skoufias, D.A., DeBonis, S., Saoudi, Y., Lebeau, L., Crevel, I., Cross, R., Wade, R.H., Hackney, D.D., and Kozielski, F. (2006). S-trityl-L-cysteine is a reversible, tight binding inhibitor of the human kinesin Eg5 that specifically blocks mitotic progression. J. Biol. Chem. *281*, 17559–17569.

Tanenbaum, M.E., and Medema, R.H. (2010). Mechanisms of centrosome separation and bipolar spindle assembly. Dev. Cell *19*, 797–806.

Tanenbaum, M.E., Macůrek, L., Janssen, A., Geers, E.F., Alvarez-Fernández, M., and Medema, R.H. (2009). Kif15 cooperates with eg5 to promote bipolar spindle assembly. Curr. Biol. *19*, 1703–1711.

Testa, J.R., and Tsichlis, P.N. (2005). AKT signaling in normal and malignant cells. Oncogene *24*, 7391–7393.

Toso, A., Winter, J.R., Garrod, A.J., Amaro, A.C., Meraldi, P., and McAinsh, A.D. (2009). Kinetochore-generated pushing forces separate centrosomes during bipolar spindle assembly. J. Cell Biol. *184*, 365–372.

Vanneste, D., Takagi, M., Imamoto, N., and Vernos, I. (2009). The role of Hklp2 in the stabilization and maintenance of spindle bipolarity. Curr. Biol. *19*, 1712–1717.

Walczak, C.E., and Heald, R. (2008). Mechanisms of mitotic spindle assembly and function. Int. Rev. Cytol. *265*, 111–158.

Walter, T., Held, M., Neumann, B., Hériché, J.K., Conrad, C., Pepperkok, R., and Ellenberg, J. (2010). Automatic identification and clustering of chromosome phenotypes in a genome wide RNAi screen by time-lapse imaging. J. Struct. Biol. *170*, 1–9.

Waters, J.C., Chen, R.H., Murray, A.W., and Salmon, E.D. (1998). Localization of Mad2 to kinetochores depends on microtubule attachment, not tension. J. Cell Biol. *141*, 1181–1191.

Whitehead, C.M., and Rattner, J.B. (1998). Expanding the role of HsEg5 within the mitotic and post-mitotic phases of the cell cycle. J. Cell Sci. *111*, 2551–2561.

Wilson, K.J., Gilmore, J.L., Foley, J., Lemmon, M.A., and Riese, D.J., 2nd. (2009). Functional selectivity of EGF family peptide growth factors: implications for cancer. Pharmacol. Ther. *122*, 1–8.

Zwick, E., Hackel, P.O., Prenzel, N., and Ullrich, A. (1999). The EGF receptor as central transducer of heterologous signalling systems. Trends Pharmacol. Sci. *20*, 408–412.